

## The LEGUE High Latitude Bright Survey Design for the LAMOST Pilot Survey

Yueyang Zhang<sup>1,3</sup>, Jeffrey L. Carlin<sup>2</sup>, Fan Yang<sup>1,3</sup>, Chao Liu<sup>1</sup>, Licai Deng<sup>1</sup>, Heidi Jo Newberg<sup>2</sup>, Haotong Zhang<sup>1</sup>, Sébastien Lépine<sup>4</sup>, Yan Xu<sup>1</sup>, Shuang Gao<sup>1</sup>, Norbert Christlieb<sup>5</sup>, Zhanwen Han<sup>6</sup>, Jinliang Hou<sup>7</sup>, Hsundai Lee<sup>8</sup>, Xiaowei Liu<sup>9</sup> and Kaike Pan<sup>10</sup> and Hongchi Wang<sup>11</sup>

- <sup>1</sup> Key Lab for Optical Astronomy, National Astronomical Observatories, Chinese Academy of Sciences, Beijing 100012, China ([zhangyy@bao.ac.cn](mailto:zhangyy@bao.ac.cn))
- <sup>2</sup> Department of Physics, Applied Physics, and Astronomy, Rensselaer Polytechnic Institute, 110 8th Street, Troy, NY 12180, USA ([carlij@rpi.edu](mailto:carlij@rpi.edu))
- <sup>3</sup> Graduate University of Chinese Academy of Sciences, Beijing 100049, China
- <sup>4</sup> Department of Astrophysics, Division of Physical Sciences, American Museum of Natural History, Central Park West at 79th Street, New York, NY 10024
- <sup>5</sup> University of Heidelberg, Landessternwarte, Königstuhl 12, D-69117 Heidelberg, Germany
- <sup>6</sup> Yunnan Astronomical Observatory, Chinese Academy of Sciences, Kunming 650011, China
- <sup>7</sup> Shanghai Astronomical Observatory, Chinese Academy of Sciences, 80 Nandan Road, Shanghai 200030, China
- <sup>8</sup> Academia Sinica Institute of Astronomy and Astrophysics, Taipei, China
- <sup>9</sup> Department of Astronomy & Kavli Institute of Astronomy and Astrophysics, Peking University, Beijing 100871, China
- <sup>10</sup> Apache Point Observatory, PO Box 59, Sunspot, NM 88349, USA
- <sup>11</sup> Purple Mountain Observatory, Chinese Academy of Sciences, Nanjing, Jiangsu 210008, China

**Abstract** We describe the footprint and input catalog for bright nights in the LAMOST Pilot Survey, which began in October 2011. Targets are selected from two stripes in the north and south Galactic Cap regions, centered at  $\delta = 29^\circ$ , with  $10^\circ$  width in declination, covering right ascension of  $135^\circ$ - $290^\circ$  and  $-30^\circ$  to  $30^\circ$  respectively. We selected spectroscopic targets from a combination of the SDSS and 2MASS point source catalogs. The catalog of stars defining the field centers (as required by the Shack-Hartmann wave-front sensor at the center of the LAMOST field) consists of all  $V < 8^m$  stars from the Hipparcos catalog. We employ a statistical selection algorithm that assigns priorities to targets based on their positions in multidimensional color/magnitude space. This scheme overemphasizes rare objects and de-emphasizes more populated regions of magnitude and color phase space, while ensuring a smooth, well-understood selection function. A demonstration of plate design is presented based on the Shack-Hartmann star catalog and an input catalog that was generated by our target selection routines.

### 1 INTRODUCTION

Following a two-year commissioning period, a Pilot Survey with the LAMOST telescope (also known as Guo Shou Jing telescope, GSJT; see Zhao et al. 2012 for an overview) began in October 2011. The LAMOST Pilot Survey, which will continue through the end of spring 2012, is an opportunity to test systems in survey mode while also obtaining valuable science data. The Pilot Survey is conducted in

preparation for the main LAMOST survey, which will begin in late 2012. The survey consists of two main components: LEGUE (LAMOST Experiment for Galactic Understanding and Exploration) will obtain spectra of millions of stars for the study of structure and substructure in the Milky Way, and LEGAS (LAMOST ExtraGalactic Surveys) is a survey of galaxies and QSOs. The unique design of the telescope (Cui et al. 2012), with a 3.6 – 4.9 meter aperture (depending on the direction in which the telescope is pointing) and a 5°-diameter focal plane populated with 4000 robotically positioned optical fibers, opens up new opportunities for large-scale spectroscopic surveys (Zhao et al. 2012). This combination of a large field of view and large aperture enables LAMOST to efficiently survey huge contiguous areas of sky to faint magnitudes.

In this work, we focus on the Galactic structure portion of the survey, or LEGUE. The LEGUE survey itself is split into two survey modes – one for observations on bright nights, and another on dark nights – with separate input target catalogs. The bright targets are also observed on dark/gray nights when the sky transparency is low. For the Pilot Survey, bright nights are defined as  $\pm 5$  nights around the full moon, dark nights as  $\pm 5$  nights around new moon, and grey time is in between. The design of the dark nights survey, which focuses on faint stars to study the Galactic halo, is discussed in Yang et al. (2012). During the Pilot Survey, an additional six nights are set aside for system engineering tasks, from 5-7 and 20-22 nights after new moon. Here we discuss the survey that was designed to take advantage of the bright and grey time during the LAMOST Pilot Survey.

On the bright nights, relatively bright ( $r \leq 16.5^m$ ) stars are observed in three different regions of sky: a low-latitude region near the Galactic anticenter (GAC), a Galactic disk region, and a constant-declination stripe at  $\delta \sim 29^\circ$ . In this paper we describe the design of the  $\delta \sim 29^\circ$  stripe, leaving discussion of the disk survey design to another work (Chen et al. 2012). Targets for the anticenter portion of the survey are being selected from a separate input catalog using data from the Xuyi photometric survey (Liu et al. 2012, in prep.), and will thus be described elsewhere. We discuss the selection of the areas to be observed and the selection of targets based on both Sloan Digital Sky Survey (SDSS; York et al. 2000) and Two Micron All-Sky Survey (2MASS; Skrutskie et al. 2006) photometry.

Bright targets are observed when the moon is bright or when the atmospheric transparency is poor. Due to poor weather conditions at the site,  $\sim 80\%$  of the telescope time is devoted to observing bright targets (see Deng et al. 2012, Yao et al. 2012 for discussion of the site conditions and sample survey strategies). During the Pilot Survey over 1 million spectra of bright stars will be obtained, with more than 5 million bright targets to be observed during the main LAMOST survey. It is thus important to test targeting strategies for optimizing the selection of objects of particular scientific interest to the collaboration, and to explore the effectiveness of the Survey Strategy System (SSS) of LAMOST at covering the sky uniformly. The Pilot Survey allows us to explore these (and other issues) while simultaneously gathering data for studies of Milky Way structure.

The structure of this paper is as follows: Section 2 discusses the construction of the overall sky catalog used for targeting and the selection of bright central guide stars for active optics corrections, especially focusing on particular elements that are unique to the bright nights survey. The design and target selection to generate the catalog to be input to the targeting software is discussed in Section 3. Section 4 compares the input magnitude and color distributions to those of the actual targets that are fed to fibers in an observing plate. Finally, we conclude with a brief summary of the bright nights survey design.

## 2 DATA AND TARGET SELECTION

The footprint of the bright nights survey is shown in equatorial ( $\alpha, \delta$ ) coordinates in Figure 1. The magenta shape is the disk survey region centered on the Galactic plane (i.e.,  $b = 0^\circ$ ), which will be discussed in another paper (Chen et al. 2012). The blue and green stripes in Figure 1 are centered at a declination of  $29^\circ$ . The green stripe is located at low ( $b < 30^\circ$ ) Galactic latitudes in the Galactic anticenter region. This stripe is mostly outside the SDSS footprint, and thus requires a different source of photometry and astrometry for LAMOST target assignment. Target selection for the anticenter region is being done based on photometry from the Xuyi Schmidt Telescope Photometric Survey of the Galactic

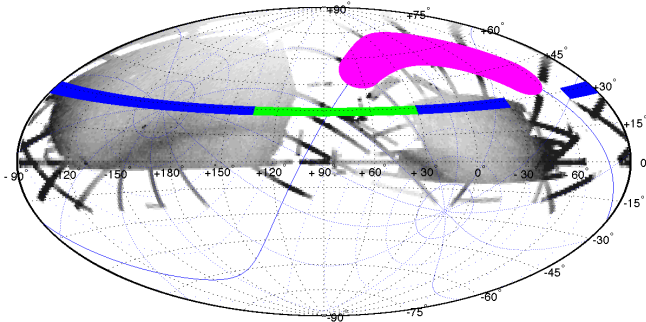


**Fig. 1** The footprint of the LAMOST bright nights survey (colored regions) in equatorial coordinates overlaid on a starcount map from SDSS photometry. The magenta part is the disk survey region centered on the Galactic plane. The blue stripes are located in the North Galactic Cap (north stripe) and the South Galactic Cap (south stripe). The green stripe is the anticenter region at low Galactic latitudes ( $|b| < 30^\circ$ ).

Anti-center (XSTPS-GAC). The Xuyi survey provides uniform photometry to  $i \sim 19^m$  in a  $\sim 3600 \text{ deg}^{-2}$  region in the Galactic anticenter, from  $150^\circ < l < 210^\circ$  and  $-30^\circ < b < 30^\circ$ . LAMOST plates were designed differently in this anticenter region than in the rest of the LEGUE survey; the target selection for the anticenter portion of the LEGUE survey will be discussed elsewhere. The blue stripes in Figure 1 are located in the northern Galactic Cap (north stripe) and in the southern Galactic Cap (south stripe). In this paper we discuss target selection for these two blue regions only; the disk and anticenter regions will be discussed elsewhere.

The constant declination stripe was placed at  $\delta = 29^\circ$  in part because the unique design of LAMOST makes this the optimal direction to point the telescope in terms of image quality. Mirror A, which acts as a Schmidt corrector despite being the first element in the optical path, is the steerable element that is pointed to targeted regions on the sky. Mirror B (the spherical Schmidt “primary”) is fixed at  $25^\circ$  above the horizon. Because the latitude at the site is  $\sim 40^\circ$ , for Mirrors A and B to be aligned, Mirror A would have to be pointed to  $\delta \sim -25^\circ$ . Therefore, when Mirror A is pointed away from  $\delta \sim -25^\circ$  the effective collecting area decreases and the images become distorted. This means that less light goes down the 3.3-arcsecond fibers at higher declinations. In practice, the telescope cannot point below  $\delta = -10^\circ$ . While this declination produces the best image quality based on the optics, it is at low altitude from the LAMOST site, making the atmospheric distortion significant. In practice, the optimal telescope performance is achieved at declinations near  $25^\circ$ . The stripe at  $\delta \sim 29^\circ$  also creates a region of contiguous observations that passes through the Galactic anticenter when integrated with the (XuYi-selected) anticenter catalogs and the LEGUE dark nights data. The width of the north and south stripes is  $10^\circ$ , spanning  $24^\circ < \delta < 34^\circ$ . The right ascension range of the north stripe is  $135^\circ - 290^\circ$ , and the south stripe covers right ascensions from  $-30^\circ$  to  $30^\circ$ .

Photometry from SDSS DR8 (Aihara et al. 2011) was used for target selection in the blue stripes because it provides a uniform dataset covering the entire region of interest. This choice was also motivated by a desire to keep the bright and faint surveys as similar as possible; targets for the LEGUE faint star survey (Yang et al. 2012) were also selected from SDSS, so that when the bright and faint surveys are combined, they will provide a relatively complete and uniform survey. However, the bright magnitude limit at which SDSS photometry saturates is  $g \sim 14^m$  (Yanny et al. 2009). To extend the survey

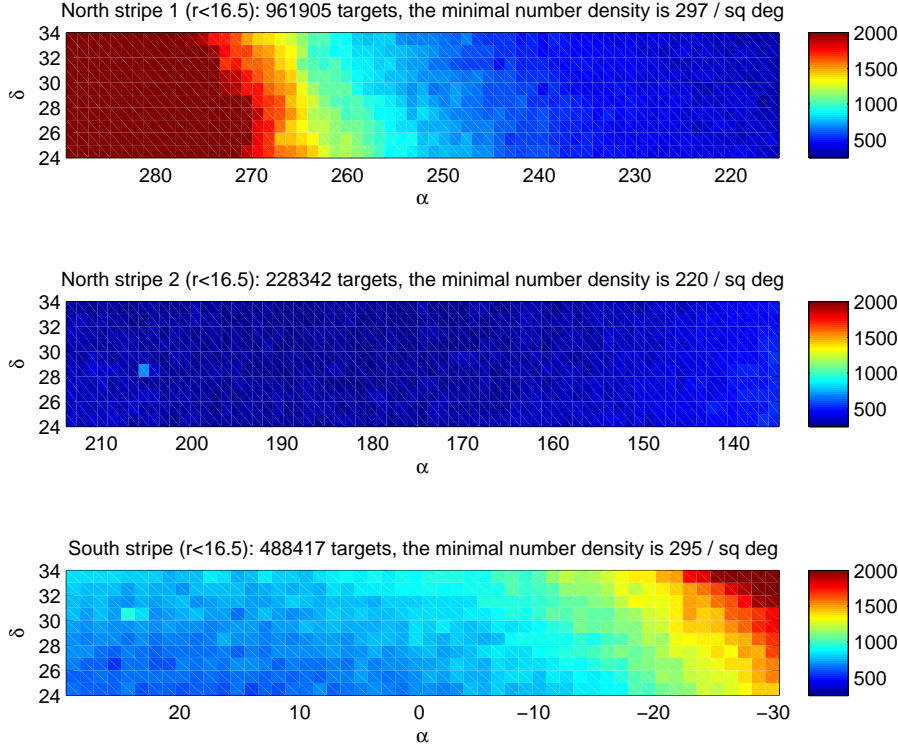


**Fig. 2** The stellar number density of the north and south stripes, including all stars from 2MASS that do not have SDSS counterparts, as well as SDSS stars with  $r < 16.5^m$ . The number density in the north stripe is  $\sim 300 \text{ deg}^{-2}$  in most of the sky near the North Galactic Pole. The lowest number density in the north stripe is  $220 \text{ deg}^{-2}$ . The number density in the south stripe is  $\sim 600 \text{ deg}^{-2}$  in high latitude areas and can reach above  $1500 \text{ deg}^{-2}$  near the plane. The lowest number density in the south stripe is  $295 \text{ deg}^{-2}$ .

to brighter magnitudes, providing more targets, we supplemented the SDSS catalog with near-infrared photometry from the 2MASS point source catalog.

The input catalog for the bright survey consists three subgroups with different magnitude information: 1. targets with only SDSS photometry; 2. targets with only 2MASS photometry; 3. targets with both SDSS and 2MASS photometry. Initially, we intended to impose a magnitude limit of  $r < 16.5^m$  for targets on bright plates. Figure 2 shows the density of targets selected in this way for both the north and south stripes. The number density of the north stripe is shown in the upper and middle panels of Figure 2 and the bottom panel shows the number density of the south stripe. The color-coding in the figure represents the stellar density of available targets in each square degree of sky. The total stellar density including all 2MASS stars and  $r < 16.5^m$  SDSS candidates is less than  $300 \text{ deg}^{-2}$  for much of the high-latitude regions in the north stripe. The LAMOST fiber assignment program typically requires three times the fiber density of candidates as input in order to fill all of the available fibers; this requires an input catalog of density  $600 \text{ stars deg}^{-2}$ . Obviously this density is not achievable for bright stars at high latitudes.

LAMOST spectra cover a wide wavelength range of  $3700 < \lambda < 9100 \text{ \AA}$ , so that some stars with extremely blue or red colors that are fainter than magnitude 16.5 in  $r$  will have enough flux to obtain useful measurements in the blue or red regions of the spectra. Thus, to increase the number of available

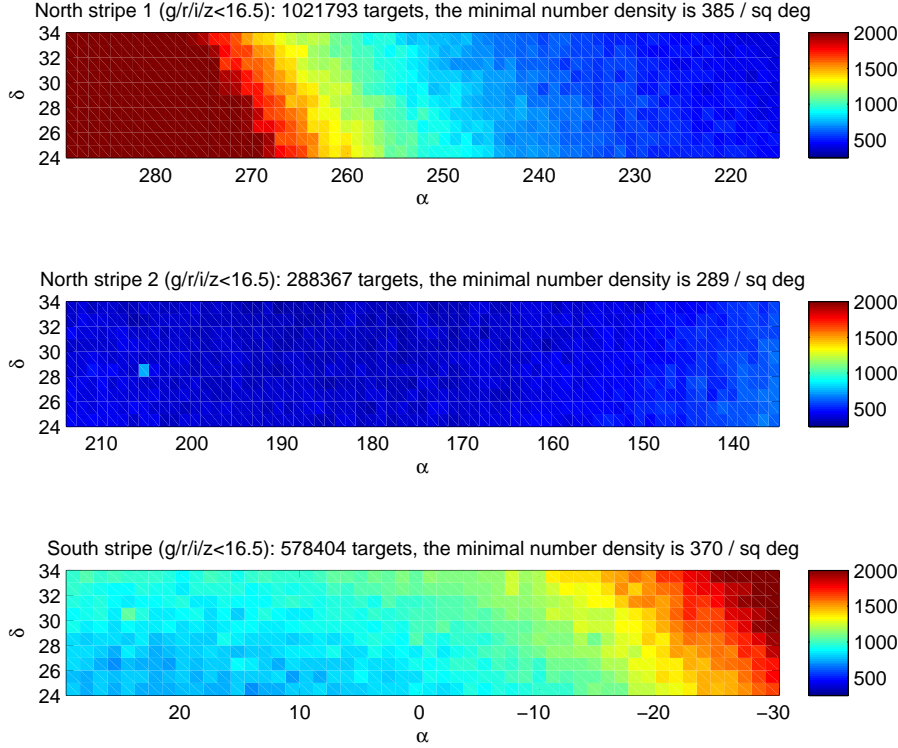


**Fig. 3** Stellar number density in the north and south stripes including all stars with  $g$ ,  $r$ ,  $i$ , or  $z$  magnitudes less than  $16.5^m$ , and all 2MASS stars at the bright end. The number density in the north stripe (shown in the upper and middle panels) is  $\sim 400 \text{ deg}^{-2}$  in most of the sky near the North Galactic Pole, with a minimum number density of  $289 \text{ deg}^{-2}$ . The number density in the south stripe (the bottom panel) is  $\sim 600 \text{ deg}^{-2}$  in high latitude areas and can reach above  $1500 \text{ deg}^{-2}$  at lower latitudes. The lowest number density in the south region is  $370 \text{ deg}^{-2}$ .

targets for the bright plates, we included stars with magnitudes brighter than  $16.5^m$  in  $g$ ,  $r$ ,  $i$ , or  $z$ -bands. For example, an M-dwarf with a red  $r-i$  color of  $r-i = 1.2^m$  and  $i = 16.3^m$  would have  $r = 17.5^m$ , but may be bright enough to provide ample flux for measurement at red (i.e.,  $i$  and  $z$ -band) wavelengths. Thus the faint magnitude limit employed for target selection in the bright survey plates is

$$g < 16.5 \mid r < 16.5 \mid i < 16.5 \mid z < 16.5 \quad (1)$$

where the “ $\mid$ ” denotes “or” (i.e., only one or more of these criteria must be met for a star to be included).

The faint magnitude limit for targets with only 2MASS photometry is the same as the magnitude limit of 2MASS point source catalog:

$$J < 15.8 \ \& \ H < 15.1 \ \& \ K_s < 14.3. \quad (2)$$

These magnitude selection criteria were chosen to ensure that the star number density is high enough that most fibers can be occupied with targets, no matter where the field of view is placed. The lowest number density in the north stripe, which appears near the northern Galactic pole, is  $\sim 290 \text{ deg}^{-2}$ , while the lowest number density in the south stripe is  $\sim 370 \text{ deg}^{-2}$  (Figure 3).

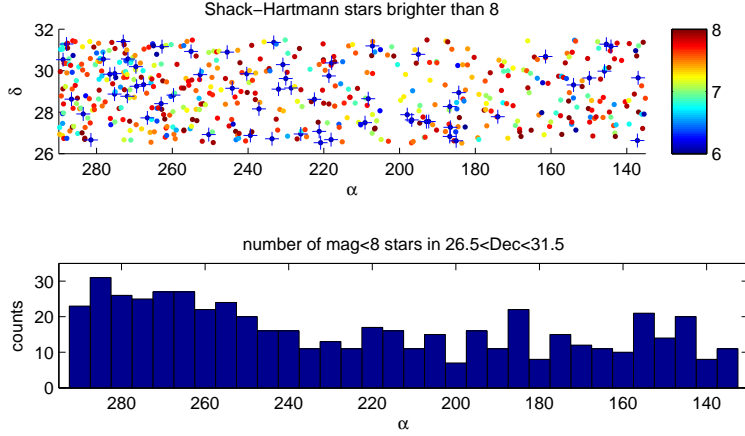


**Fig. 4** The Shack-Hartmann star distribution of the north stripe along right ascension, considering stars with  $V < 8^m$ . Stars with  $V < 6^m$  are highlighted by “+”. The lower panel shows that there are enough stars to make sure there are plates available to observe for a given right ascension. Note, however, that on bright nights when the sky background is elevated, the faint limit for Shack-Hartmann stars is between 6-7th magnitude, which limits the choice of available plate centers.

Active optics on LAMOST requires that each plate be centered on a bright,  $V < 8$  star that is fed to the Shack-Hartmann wavefront sensor. For this purpose, we generated a catalog of potential Shack-Hartmann stars from the Hipparcos catalog (Perryman et al. 1997). The declination range of the Shack-Hartmann catalog is  $26.5\text{--}31.5^\circ$ , which is centered at the same declination ( $29^\circ$ ) and covers half the width of the north and south stripes. A field centered on a star with higher or lower declination would not fall completely within our desired observing footprint. The distribution of these stars is seen in Figures 4 and 5, color-coded by their Hipparcos  $V$  magnitudes. Stars with  $V < 6^m$  are highlighted by “+”. For the bright survey, where plates are often being observed in periods of elevated sky background (either due to moonlight or clouds/haze), it is often necessary to use a brighter central star (say,  $V \sim 6^m$ ) in order for the Shack-Hartmann system to measure sufficient flux above background for image correction. As can be seen in Figures 4 and 5, limiting the central star to  $V < 6^m$  places strict limits on the available plate centers.

The stripes and their corresponding Shack-Hartmann catalogs were designed to cover a  $10^\circ$  declination range to ensure that there are always plates available to observe near a given right ascension. Because LAMOST is a fixed meridian telescope, it is essential that multiple plates are available at each right ascension for flexibility in plate selections.

The selection function can be assessed by the simulation of Galactic models like Sharma et al.’s synthetic survey in the future.

### 3 SKY TO INPUT CATALOG

The LEGUE Pilot Survey target selection algorithm is presented in detail in Carlin et al. (2012). Here we give a brief overview and some details that are specific to the bright-star portion of the Pilot Survey, but the global target selection routine is similar to that for the faint Galactic halo portion of the Pilot Survey. The goal is to overemphasize relatively rare stars in sparsely-populated regions of parameter space while sampling large numbers of more common types of stars.

The LAMOST fiber assignment algorithm of SSS performs optimally with an input catalog of roughly three times the desired target density. There are 200 fibers per square degree in the LAMOST



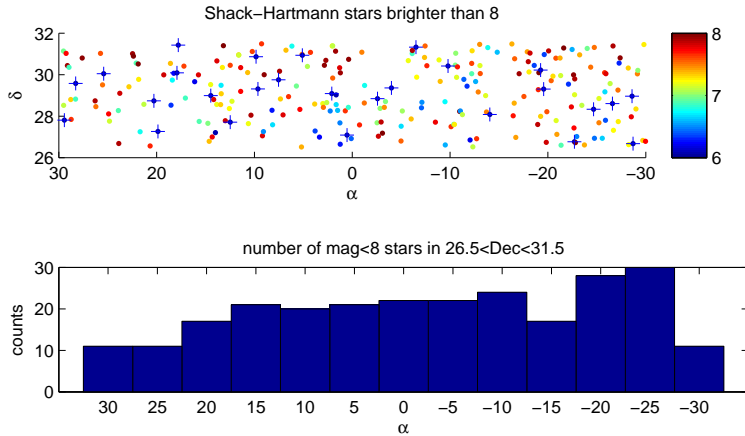


**Fig. 5** As in Figure 4, but showing the Shack-Hartmann star distribution of the south stripe along right ascension, considering stars with  $V < 8^m$ . There are more stars available in the southern sky, making the plate design more flexible in this region.

focal plane, so the input catalogs should ideally contain at least 600 candidates per square degree. As discussed in Section 2 and seen in Figure 3, this target density cannot be achieved at high latitudes in a sample that is limited to magnitudes brighter than  $16.5^m$ . Thus we choose to create an input catalog that contains all stars between  $14^m < r < 16.5^m$ , and all stars from 2MASS that do not have an SDSS counterpart (i.e., mostly stars brighter than  $r = 14^m$ ). The catalog that is given to the fiber assignment program is generated using the algorithm outlined in Carlin et al. (2012). This algorithm selects candidates based on a general probability function

$$P_{j,D} = \frac{K_D}{[\Psi_0(\lambda_i)]_j^\alpha} f_i(\lambda_i) \quad (3)$$

where  $\lambda_i$  denotes any observable (i.e., photometry, astrometry, or any combination of observed quantities) and  $\Psi_0(\lambda_i)$  is the statistical distribution function of the observable  $\lambda_i$ . The  $K_D$  term is a normalization constant to ensure that the probabilities sum to one. The  $f_i(\lambda_i)$  term is an optional function that can be used to overemphasize targets in particular regions of parameter space; this function is not used (i.e.,  $f_i(\lambda_i) = 1$ ) in the bright survey. The density of stars is calculated in multidimensional observable space, and the candidates are weighted by a power of this “local density”. The exponent  $\alpha$  that determines the weighting is typically between 0 and 1; when  $\alpha = 0$ , the probability of each target to be selected is the same (i.e., a random selection) and the distribution of the selected sample will be the same as that of the input sample. When  $\alpha = 1$ , the probability of a target to be selected is inversely proportional to the local density in the observable space, producing a selected sample that is evenly distributed across the observable space. As a result, the rare objects are over-emphasized. For the LEGUE bright survey targets, we selected an intermediate case of  $\alpha = 1/2$  (i.e., weighting by the inverse square root of the local density), which emphasizes the selection of rare objects but keeps a large number of stars from higher-density regions in the observables. For stars having SDSS magnitudes, we used  $r, g - r$ , and  $r - i$  to calculate the local density for targeting, and for those with 2MASS photometry only, density was defined in  $J, J - H, J - K$  parameter space. Unlike the dark night survey of faint targets (Yang et al. 2012), we did not add any linear weights (i.e.,  $f_i = 1$ ) in color or magnitude to the bright survey selection criteria.

Because the selection probabilities for stars appearing in SDSS were generated separately from those appearing only in 2MASS, the two resulting catalogs were concatenated and renormalized so that

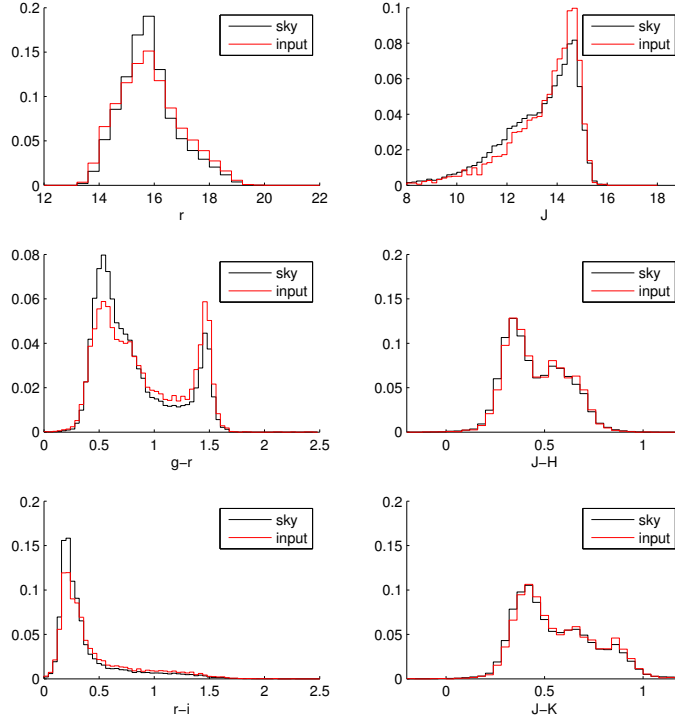


**Fig. 6** Magnitude and color distributions of stars in a low Galactic latitude ( $b \approx -20^\circ$ ) sky area and its corresponding input catalog. The left column depicts all stars with SDSS photometry, and the right includes stars with only 2MASS data. Black lines represent the distribution of all the original data in the sky area, and red lines are 600 candidates  $\text{deg}^{-2}$  selected using the target selection method discussed in the text. Targets to be input to the fiber assignment program contain a smaller fraction of relatively common turnoff stars (at  $0.3^m < g-r < 0.6^m$ ), with redder stars overemphasized. The 2MASS distributions of “sky” and “input” stars are similar because nearly all of the small number of available targets are selected by the targeting routine.

they sum to one. The resulting catalog was then used to select target candidates to give to the fiber assignment program.

As is evident in Figures 2 and 3, the input catalog density at high Galactic latitudes is less than  $400 \text{ deg}^{-2}$ , even after including bright 2MASS targets with the SDSS stars. Thus, the selection of 600 stars per square degree is not possible at high latitudes, and all available stars will be included in the catalog input to the SSS fiber assignment program. At low latitudes, the high density of available targets means that we must sub-sample using the algorithm described above. Here we illustrate the effect of the target selection algorithm by comparing the magnitude and color distributions of the original data on the sky and the selected input catalog for a low-latitude ( $|b| \sim 20^\circ$ ) field. This example field is at  $330^\circ < \alpha < 336^\circ$  (i.e.,  $-30^\circ < \alpha < -24^\circ$ ),  $28^\circ < \delta < 34^\circ$ , with  $b \approx -20^\circ$ . Figure 6 shows the magnitude and color distributions of the original data and the selected input catalog from the same sky area for this low-latitude field. Panels show stars with SDSS photometry in the left column and those with only 2MASS photometry in the right column. The effect of the overemphasis on relatively rare stars is evident; this is especially clear in the middle left panel, which shows the  $g-r$  color



distribution. The selected candidates (the red histogram) have a lower peak near the main sequence turnoff locus ( $g - r \sim 0.3 - 0.6^m$ ) than the overall distribution, a slight excess at intermediate colors ( $0.6^m < g - r < 1.3^m$ ), and a clear excess of M-type stars at  $g - r \sim 1.5^m$ . The M-star excess arises because of the wide spread of M-dwarf  $r - i$  colors at a nearly constant  $g - r \sim 1.5^m$ ; this causes the density of M stars to be “diluted” in three-dimensional  $r, g - r, r - i$  space (relative to the piling up in  $g - r$  alone), giving the metal-poor tail (at red  $r - i$  colors) of these relatively common stars a high probability of selection. There are only a small number of bright 2MASS candidates available outside of the Galactic disk region, so in most areas the “sky” and “input” distributions in  $J, J - H, J - K$  will look nearly identical.

#### 4 INPUT CATALOG TO PLATE DESIGN

When SSS designs a plate for observations, it assigns targets of the input catalog to fibers depending on priorities given to targets in the input catalog. For the Pilot Survey, priorities were assigned in a way that roughly reproduces the desired distribution of targets according to the assignment probabilities calculated for each star (for more details, see Carlin et al. 2012). In principle, the magnitude and color distributions of a designed LAMOST plate should be the same as those of the input catalog in the corresponding sky area. To show this, we simulated the generation of a plate using SSS for the low-latitude field illustrated in Figure 6. The center of the simulated plate and the corresponding input catalog is  $(\alpha, \delta) = (333^\circ, 31^\circ)$ . The plate is a circle with a radius of  $2.5^\circ$  centered on an available Shack-Hartmann star. The input catalog is a rectangular box with  $330^\circ < \text{RA} < 336^\circ$ ,  $28^\circ < \delta < 34^\circ$ , the same area as exemplified in Section 3. Figure 7 shows the input catalog as a solid black line, and the targets selected by SSS for the plate as a red line. Other than minor statistical fluctuations, this figure shows that the magnitude and color distribution of the generated plate represents the input catalog well. We are thus confident that our target selection process is yielding the desired distribution of targets in the final survey design.

Based on the input catalog and the list of available Shack-Hartmann stars, we use SSS to simulate a series of plates that covers the north and south strips along  $\delta \sim 29^\circ$ . Plates are placed with a little overlap on the edge; in this simulation, meant for illustration only, there was little concern about optimally tiling regions of sky. Real observational constraints and weather conditions are not considered. On a nightly basis, these will be important factors in the design of plates due to the limited range about the meridian to which LAMOST can point. Figure 8 shows the results of this simple simulation – the upper panel illustrates a string of plates in the north Galactic cap, and the lower panel, the southern cap. The figure shows the density of stars selected for observation by SSS in 0.25-degree squares on the sky. Because of the low number density of available stars in the north Galactic pole, the mean density of those plates with high Galactic latitudes is  $\sim 160 \text{ stars deg}^{-2}$ , falling short of the  $200 \text{ deg}^{-2}$  fiber density of LAMOST. The declining stellar density in the north strip is evident as a decreasing target density with increasing right ascension in the upper panel. Table 1 and Table 2 present the numbers of targets along with the coordinates of the plates’ centers for the north and south stripe respectively.

#### 5 SUMMARY

In this paper, we described the input catalog for observations on bright nights of the LAMOST Pilot Survey. The sky coverage of the survey consists of a contiguous stripe at roughly constant declination of  $\sim 29^\circ$ . We discussed details of the plate design, which included a combination of SDSS and 2MASS photometry. The input catalog of the bright nights survey consists of SDSS stars brighter than  $16.5^m$  and all 2MASS point sources brighter than the limiting magnitude ( $r \sim 14^m$ ) of SDSS. The target selection method is based on pre-assigned priorities, which weight stars by the inverse square root of the “local density” in  $r, g - r, r - i$  (or  $J, J - H, J - K$  for those having only 2MASS magnitudes) to overemphasize rare objects and de-emphasize the objects in more populated regions of magnitude and color phase space. We illustrate the differences between the magnitude and color distributions of stars selected by our target selection method and the overall distribution for a given region of sky.

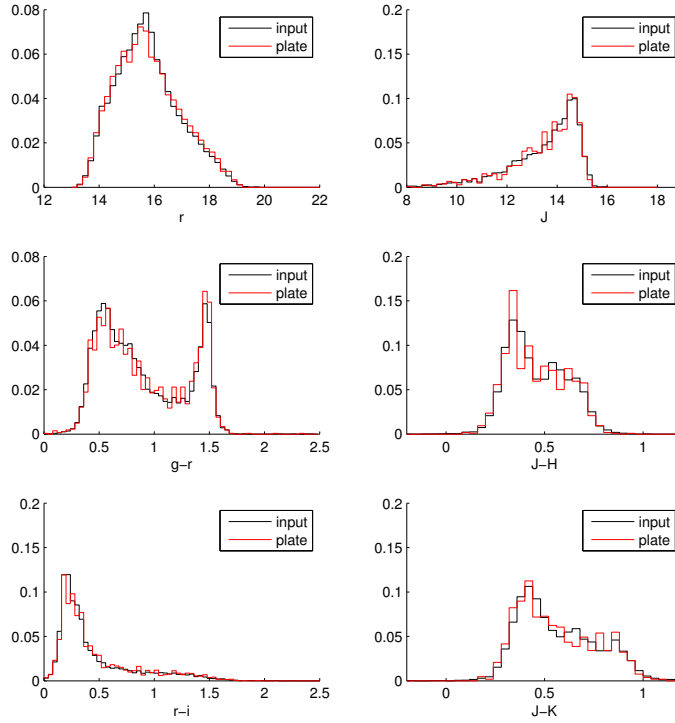


**Fig. 7** The magnitude and color distribution of the simulated plate used in Figure 6 and its corresponding input catalog. The center of the simulated plate and the corresponding input catalog is  $(\alpha, \delta) = (333^\circ, 31^\circ)$ . The plate is a circle with a radius of  $2.5^\circ$ . The input catalog is a  $6^\circ \times 6^\circ$  rectangular box. Modulo some statistical fluctuations, the distribution of the targets selected for a plate are nearly identical to the input catalog.

Overall, the LAMOST/LEGUE Pilot Survey will obtain 1-2 million stellar spectra of bright stars (in addition to the faint stars from the other components of the survey) spanning a range of Galactic latitudes. These spectra will yield numerous scientific results while also providing valuable test data for refinement of LAMOST survey operations.

**Acknowledgements** This work is partially supported by National Natural Science Foundation of China (NSFC) through grant No.10573022, 10973015, 11061120454 and by Chinese Academy of Sciences (CAS) through grant GJHZ20081, and the US National Science Foundation through grant AST-09-37523.

## References

- Aihara, H., Allende Prieto, C., An, D., et al. 2011, *ApJS*, 193, 29  
 Carlin, J. L., Lépine, S., Newberg, H. J., et al. 2012, *Research in Astron. Astrophys. (RAA)*, in press  
 Chen, L., Hou, J., Yu, J., et al. 2012, *Research in Astron. Astrophys. (RAA)*, in press  
 Cui, X. Q., Zhao, Y. H., Chu, Y. Q., et al. 2012, *Research in Astron. Astrophys. (RAA)*, in press  
 Deng, L., Newberg, H. J., Liu, C., et al. 2012, *Research in Astron. Astrophys. (RAA)*, in press  
 Perryman, M. A. C., Lindegren, L., Kovalevsky, J., et al. 1997, *A&A*, 323, 49

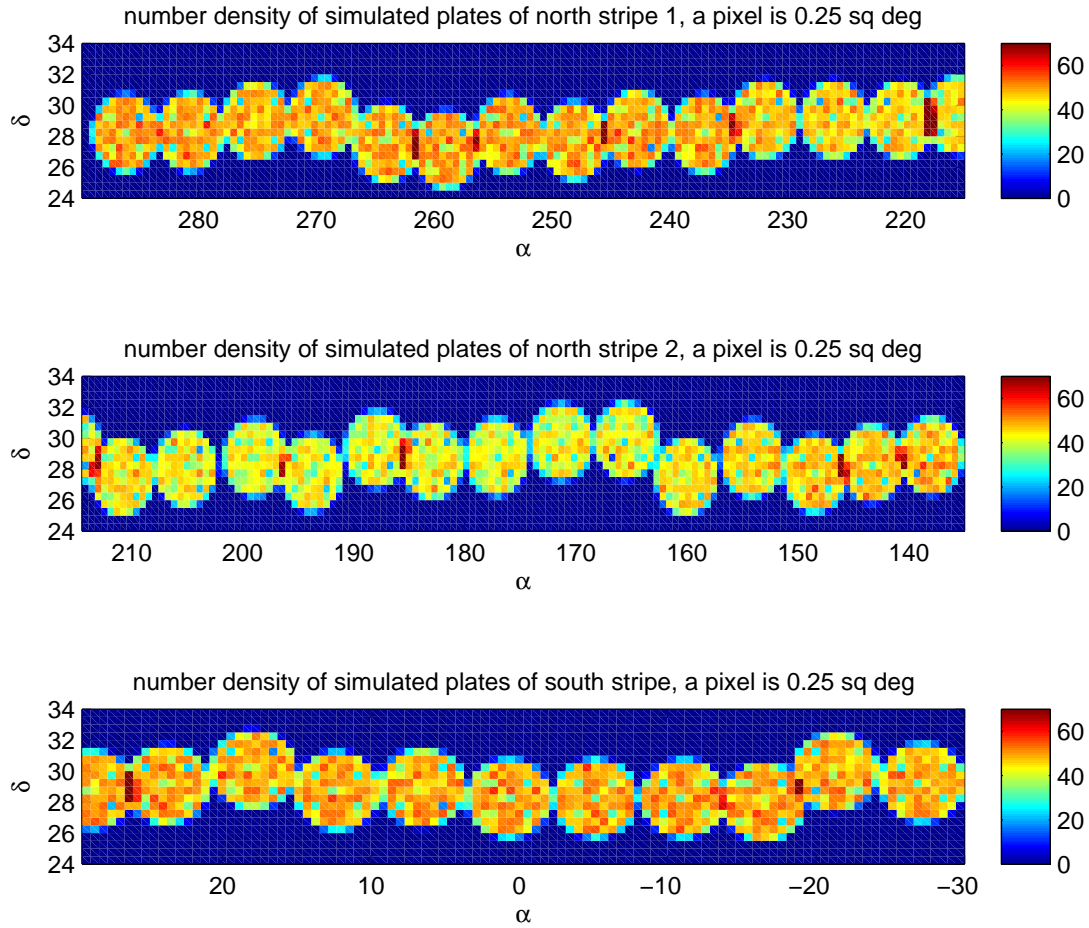


**Fig. 8** A simple demonstration of how plates could be placed along the north and south stripes. Plates are generated by running a large input catalog based on our target selection criteria through a SSS simulation, with the center of each plate determined by the available Shack-Hartmann stars. The circles represent LAMOST plates, with the 0.25-degree squares giving the density of selected stars in each plate. Note that the density of stars in the NGC (upper panel) region drops with increasing latitude (roughly along  $\alpha$  in this stripe), so that fewer than 200 stars  $\text{deg}^{-2}$  are observed at high latitudes.

- Sharma, S., Bland-Hawthorn, J., Johnston, K. V., et al. 2011, *ApJ*, 730, 3
- Skrutskie, M. F., Cutri, R. M., Stiening, R., et al. 2006, *AJ*, 131, 1163
- Yang, F., Carlin, J. L., Liu, C., et al. 2012, *Research in Astron. Astrophys. (RAA)*, in press
- Yanny, B., Rockosi, C., Newberg, H. J., et al. 2009, *AJ*, 137, 4377
- Yao, S., Liu, C., Zhang, H. T., et al. 2012, *Research in Astron. Astrophys. (RAA)*, in press
- York, D. G., Adelman, J., Anderson, J. E., Jr., et al. 2000, *AJ*, 120, 1579
- Zhao, G., Zhao, Y., Chu, Y., et al. 2012, *Research in Astron. Astrophys. (RAA)*, in press

**Table 1** The Numbers of Stars Targeted in the Plates Simulated along the North Stripe

plate No.	$\alpha$ of the plate center	$\delta$ of the plate center	number of targets
north 01	137.9892450	28.8715765	3685
north 02	143.3263274	28.3680181	3637
north 03	148.4965638	27.6954653	3566
north 04	154.1171840	28.6827033	3494
north 05	160.0882441	27.5252721	3416
north 06	165.4555274	29.8712896	3321
north 07	171.3191614	29.7587449	3293
north 08	177.1524763	28.7999489	3259
north 09	183.0040488	28.5364632	3253
north 10	187.9606690	29.3141653	3256
north 11	193.7844659	27.7665362	3244
north 12	198.9016961	28.7419682	3270
north 13	205.1630134	28.0651406	3348
north 14	210.8639400	27.5099545	3443
north 15	215.5584468	29.3699840	3440
north 16	220.3432808	29.0592524	3525
north 17	226.0668756	29.0785150	3584
north 18	231.9577163	29.1054916	3684
north 19	237.1434012	28.1567769	3751
north 20	242.8491569	28.4387012	3793
north 21	248.1120058	27.7094406	3771
north 22	253.7299374	28.1370510	3791
north 23	258.9954871	27.1343421	3767
north 24	264.0892623	27.5668072	3718
north 25	269.4409611	29.2479253	3805
north 26	275.1055312	28.9835392	3757
north 27	280.7169777	28.3027952	3792
north 28	286.2285437	28.1882454	3792

**Table 2** The Numbers of Stars Targeted in the Plates Simulated along the South Stripe

plate No.	$\alpha$ of the plate center	$\delta$ of the plate center	number of targets
south 01	332.8464044	29.2546550	3767
south 02	338.6976207	29.9574026	3778
south 03	343.5475406	28.0166028	3760
south 04	348.9428409	28.2479046	3791
south 05	354.8782129	28.2459536	3789
south 06	0.7101522	28.2518911	3788
south 07	6.5113298	28.9405581	3783
south 08	12.2903523	28.7193068	3804
south 09	17.9149447	30.0897296	3810
south 10	23.7578593	29.1007859	3789
south 11	28.7807900	28.7979522	2914